Eosin Y Covalently Anchored on Reduced Graphene Oxide as an Efficient and Recyclable Photocatalyst for the Aerobic Oxidation of α-Aryl Halogen Derivatives

Zhen Li, Wenfeng Zhang, Qingshan Zhao, Hanying Gu, Yang Li, Guoliang Zhang, Fengbao Zhang, and Xiaobin Fan*

State Key Laboratory of Chemical Engineering, School of Chemical Engineering and Technology, Collaborative Innovation Center of Chemical Science and Engineering, Tianjin University, Tianjin 300072, China

S *Supporting Information*

ABSTRACT: A visible-light photoredox with homogeneous catalyst-like transition metal complexes and organic dyes shows promising applications in organic synthesis. However, the practical applications of these photocatalysts are hampered by the difficulty of separating and recycling them from the reaction mixtures. In this study, we report the covalent immobilization of Eosin Y on reduced graphene oxide and demonstrate the obtained hybrid can be used as a recyclable photocatalyst with excellent catalytic performances in the aerobic oxidation of α-aryl halogen derivatives.

KEYWORDS: *Photocatalysis, graphene, Eosin Y, metal-free, covalent immobilization*
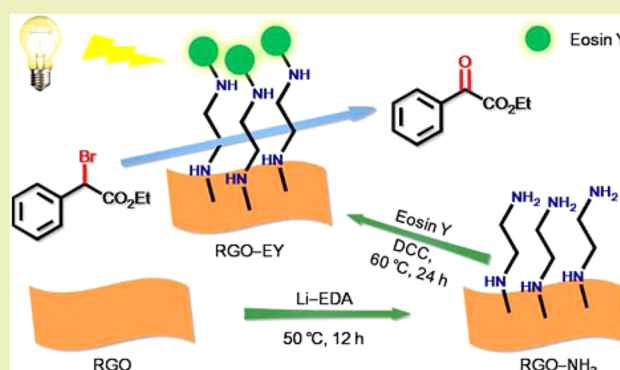
■ INTRODUCTION

Development of new, green and sustainable reaction protocols by using abundant, inexpensive, nonpolluting and endless sunlight energy has attracted significant interest in recent years. So far, a variety of elegant chemical transformations via visible-

Scheme 1. Illustration for the Preparation of RGO−EY and Its Photocatalystic Application for the Aerobic Oxidation of Benzyl Halides
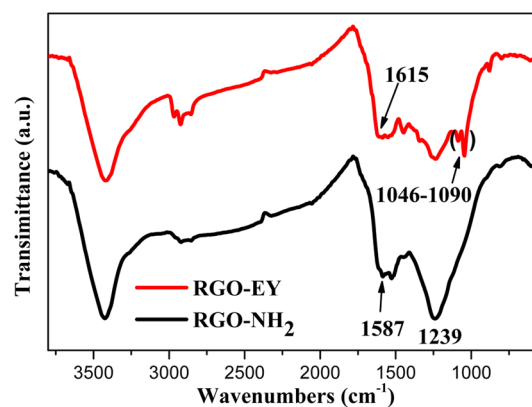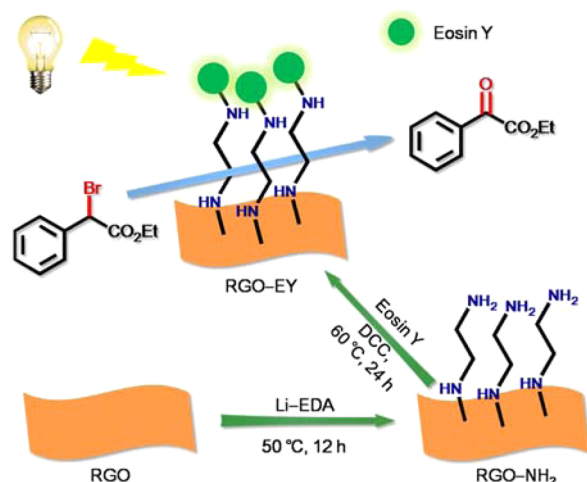

Figure 1. FTIR spectra of RGO−NH$_2$ and RGO−EY.

light photoredox have been demonstrated.[1-7] For example many tris(bipyridine) ruthenium and iridium complexes have been used as visible light photoredox catalysts in dehalogenation,[8,9] reduction,[10,11] oxidation,[12,13] cyclization,[14,15] cyclo-addition,[16,17] alkylation[18,19] and arylation[20,21] reactions. However, the high cost, potential toxicity and limited availability of these metal-based catalysts hinder their utilization in the future,
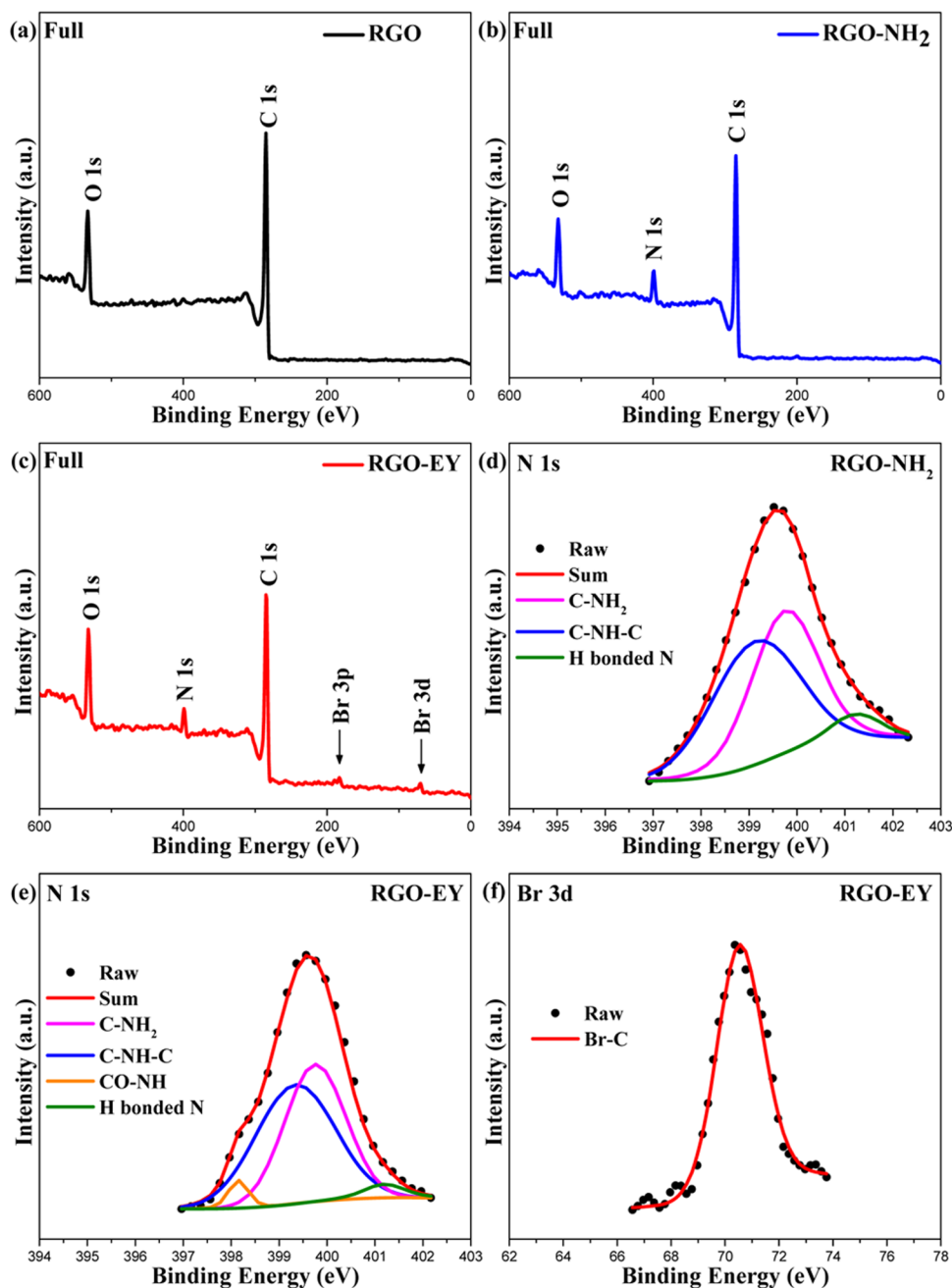
Figure 2. Full XPS spectra of (a) RGO, (b) RGO−NH₂ and (c) RGO−EY, N 1s XPS spectra of (g) RGO−NH₂ and (h) RGO−EY and Br 3d XPS spectrum of (f) RGO−EY.

whereas the cheaper metal-free organic dyes can substantially broaden the field of visible light photochemistry.[22-26] Actually, the persistent quest to introduce metal-free dyes has been successfully addressed with the use of eosin dyes.[27-34] Nevertheless, because of the difficulty in separating these dyes from homogenous system, their practical applications in chemical industry are still limited. Immobilization of dyes like Eosin Y (EY) on an appropriate support is expected to overcome this crucial problem, and traditional supports, such as TiO₂ and resin, have been investigated.[35-39]

Graphene is a new material composed of a single atomic sheet of conjugated sp² carbon atom,[40,41] which has sparked great interests in nanocatalysis[42,43]. Unlike other materials, such as inorganic solids or organic polymers, graphene has a distinctive two-dimensional structure and intriguing properties

including impressive mechanical strength and exceptional electronic and optical properties.[44-48] These properties make graphene a promising support for immobilizing dyes in photocatalysis. Nevertheless, although EY has been anchored on reduced graphene oxide (RGO) by the noncovalent interaction for visible-light photocatalysis,[49,50] it may suffer from many problems, such as dye leaching and inferior catalytic performance.

In this study, we report the covalent immobilization of EY onto the planar RGO surface by employing the primary amine functionalized RGO (RGO−NH₂) as an intermediate (Scheme 1). The obtained supported catalyst (RGO−EY) was used as a superior photocatalyst towards the aerobic oxidation of benzyl halides. The catalyst can be also easily recovered and reused with acceptable efficiency for several times.

■ EXPERIMENTAL SECTION

Preparation of Eosin Y Covalently Anchored on Reduced Graphene Oxide (RGO−EY). The amine-modified RGO (RGO−NH$_2$) was prepared by a new strategy developed by our group.[51] In brief, RGO, prepared and purified following the procedure established by Rodney S. Ruoff,[52] was functionalized with ethylenediamine (EDA) by a simple one-pot process, using a lithium ethylenediamine derivative as a nucleophilic reagent at 50 °C for 12 h. RGO−EY was synthesized by the dehydrate coupling of the carboxyl group of Eosin Y free acid (EY-FA) with the amino group of RGO−NH$_2$ using dicyclohexylcarbodiimide (DCC) as a dehydrating reagent. Briefly, 200 mg of RGO−NH$_2$, 100 mg of EY−FA and 120 mg of DCC were added into 20 mL of THF. The resultant mixture refluxed at 60 °C for 24 h. After filtration and washing with ethanol, the precipitate was dialyzed against deionized water to remove excess EY−FA and completely dried by lyophilization.

Photocatalytic Ability Toward Aerobic Oxidation. To a mixture of RGO−EY (20 mg), Li$_2$CO$_3$ (74 mg, 1 mmol) and 4-methoxypyridine (22 mg, 0.2 mmol) in DMA (15 mL) was added ethyl α-bromo(phenyl)acetate (243 mg, 1 mmol) under air atmosphere at 25 °C. The mixture was stirred under irradiation using a 24 W compact fluorescent bulb at 20 cm. After 24 h, the catalyst was separated by filtration, and the filtrate was analyzed by GC (gas chromatography).

Characterization. The samples were characterized by Fourier transform infrared spectroscopy (FTIR) (Thermo-Nicolet 380), scanning electron microscopy (SEM) (Hitachi S4800), transmission electron microscopy (TEM) (JEM-2100F), energy dispersive spectroscopy (EDS) (Hitachi S4800) and X-ray photoelectron spectroscopy (XPS) (PerkinElmer, PHI 1600spectrometer). The catalytic reactions were monitored by a GC (Agilent6890N GC-FID system).

■ RESULTS AND DISCUSSION

As illustrated in Scheme 1, to covalently immobilize the Eosin Y (EY), reduced graphene oxide (RGO) was first functionalized
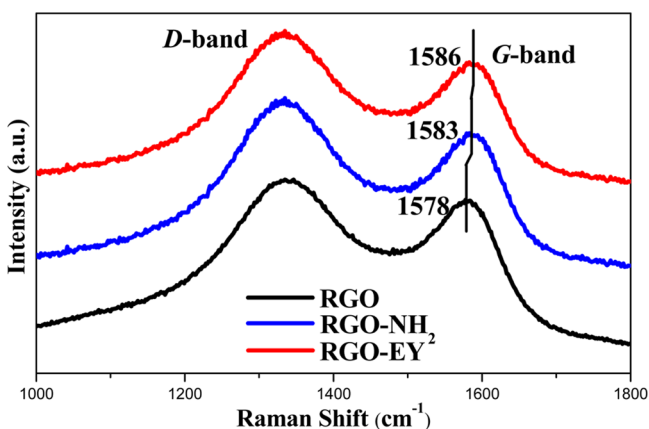

Figure 3. Raman spectra of RGO, RGO−NH$_2$ and RGO−EY.

with ethylenediamine (EDA) to obtain the amine-modified reduced graphene oxide (RGO−NH$_2$) by using a lithium ethylenediamine derivative as a nucleophilic reagent. Then, EY was introduced by the dehydrate coupling of the carboxyl group of Eosin Y free acid (EY-FA) with the amino group of RGO−NH$_2$ by using dicyclohexylcarbodiimide (DCC) as a dehydrating reagent.

Fourier transform infrared spectroscopy (FTIR) provides strong evidence for the introduction of EY onto RGO (Figure 1). Comparing the spectrum of RGO−NH$_2$ with RGO (Figure S1, Supporting Information), the presence of the N—H stretching vibration (1587 cm^{-1}) and C—N stretching
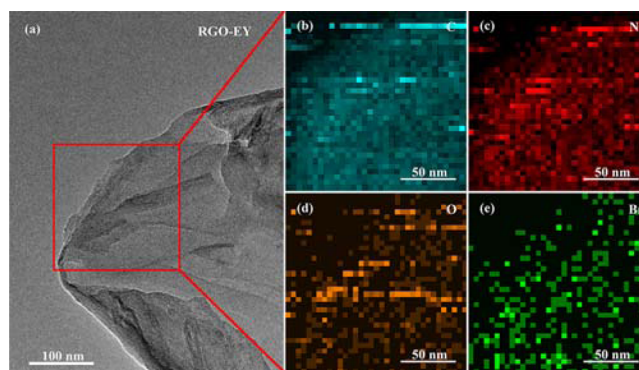

Figure 4. (a) TEM image of RGO−EY and corresponding quantitative EDS mapping of (b) C, (c) N, (d) O and (e) Br.

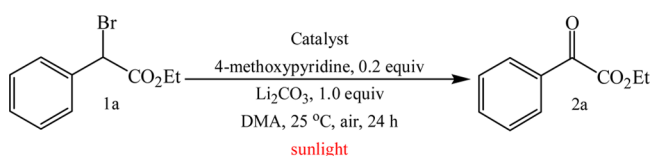**Scheme 2. Potocatalyzed Aerobic Oxidation of Ethyl α-Bromo(phenyl)acetate**

Table 1. Potocatalyzed Aerobic Oxidation of Ethyl α-Bromo(phenyl)acetate[a]

entry	catalyst	yield [%][b]	selectivity [%]
1	blank	20	41
2	EY−FA[c]	18	33
3	RGO	25	58
4	EY−FA[d]	42	66
5	RGO−EY	50	66

[a]Standard conditions: 1a (1.0 mmol), Li$_2$CO$_3$ (1.0 mmol), 4-methoxypyridine (0.2 mmol) and catalyst (20 mg) were added in DMA (15 mL) under air at 25 °C. Irradiation time using a 24 W compact fluorescent bulb at 20 cm was 24 h. [b]Calibrated yields determined by GC. [c]The reaction was carried out in the dark. [d]Using equivalent homogeneous analogue (Eosin Y, 2.90 μmol).
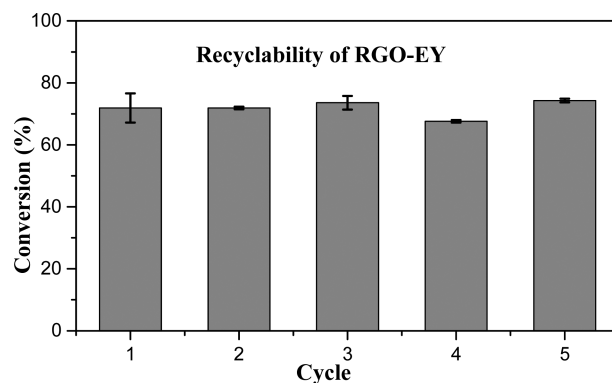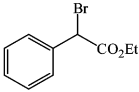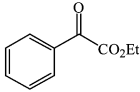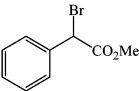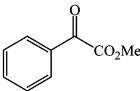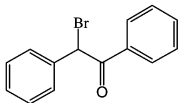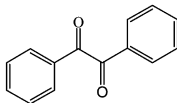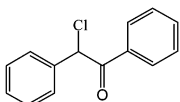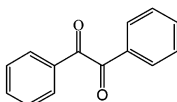

Figure 5. Recyclability of RGO−EY in aerobic photo-oxidation of benzyl halides.

vibration (1239 cm^{-1}) validate the successful introduction of terminal amines. The successful immobilization of EY is supported by the emerge of two new bands at 1615 and 1046−1090 cm^{-1}, corresponding to the vibration of C=O and C—O from EY, respectively. Note that due to the introduction of EY by the dehydrate coupling reaction, the N—H stretching

Table 2. Synthesis of α-Aryl Carbonyl Compounds 2 from 1 by RGO−EY[a]

entry	1		2		yield[%][b]	selectivity[%]
1		1a		2a	50	66
2		1b		2b	53	78
3		1c		2c	65	66
4		1d		2c	14	30

[a]Standard conditions: 1a−d (1.0 mmol), Li_2CO_3 (1.0 mmol), 4-methoxypyridine (0.2 mmol) and catalyst (20 mg) were added in DMA (15 mL) under air at 25 °C. Irradiation time using a 24 W compact fluorescent bulb at 20 cm was 24 h. [b]Calibrated yields determined by GC.

vibration and C−N stretching vibration become less prominent. Additionally, after the dehydration, the bands (at 1756, 1420 and 1211 cm^{-1}) of −COOH from EY disappear (Figure S2, Supporting Information), indicating the successful conversion of carboxyl groups into O=C—N.

The compositions of the RGO, RGO−NH$_2$ and RGO−EY were also analyzed by X-ray photoelectron spectroscopy (XPS). Compared with the RGO precursor (Figure 2a), new signals of N 1s from the EDA (Figure 2b,c) and Br signal from EY (Figure 2c) clearly emerge in the obtained RGO−NH$_2$ and RGO−EY. Note that the element atomic ratio of Br in the final RGO−EY is 0.77%, presenting an EY loading content of 0.15 mmol·g^{-1} (weight percentage of 9.3%). The successful grafting of NH$_2$ and subsequent loading of EY are also supported by corresponding XPS spectra of N 1s, C 1s and Br 3d. As can be seen from Figure 2d, the XPS spectra of N 1s from RGO−NH$_2$ can be deconvoluted into three peaks, which are attributed to C—NH—C (399.3 eV), C—NH$_2$ (399.7 eV) and hydrogen bonding between primary amine groups (401.2 eV). After EY is loaded (Figure 2e), however, the C—NH$_2$ and hydrogen bonding decrease obviously, with a new peak appearing at 398.2 eV, corresponding to O=C—N. The deconvoluted C 1s spectrum for RGO−EY also revealed the appearance of O=C—N at 285.7 eV (Figure S3, Supporting Information). These observations certify the primary amine group is partially transformed to amide group, and suggest EY is successfully introduced.

Raman spectroscopy plays an important role in the study and characterization of functionalized graphitic materials, due to its ability to detect the changes in structure. In general, the Raman spectrum of graphene possesses two main features. The G band arises from the first-order scattering of the E_{2g} phonon of sp^2 C atoms (at around 1600 cm^{-1}), and the D band arising from a breathing mode of κ-point photons of A_{1g} symmetry (at around 1300 cm^{-1}).[53] The Raman spectra of RGO, RGO−NH$_2$ and RGO−EY (Figure 3) show an obvious step-by-step blue shift of the G band from 1578 to 1583 and 1586 cm^{-1}, presumably due to the gradually increased compressive local stress induced by the introduction of primary amine and EY. And the $I_{(D)}/I_{(G)}$

intensity ratio grows from 1.95 to 2.00 and 2.51, indicating an increased disordered structure caused by the introduction of functional groups into the sp^2 carbon basal plane.

The morphology of obtained RGO−EY was determined by transmission electron microscopy (TEM). Figure 4a shows that the RGO−EY presents a wrinkled structure. Corresponding quantitative energy dispersive X-ray spectroscopy (EDS) mapping was employed to investigate the density and distribution of EY on RGO. It can be seen in Figure 4b−e that the elements C, N, O and Br are homogeneously dispersed on the whole surface of RGO−EY, indicating uniform distribution of EY on RGO. Similar results were observed in scanning electron microscopy (SEM) and its corresponding EDS mapping (Figure S4, Supporting Information). The quantitative EDS result of Br reveals an EY loading content that approximates the XPS result (Figure S5 and Table S1, Supporting Information).

To test the catalytic performance and reusability of the obtained RGO−EY, the aerobic oxidation of benzyl halide was studied (Scheme 2), and several control experiments were performed for comparison purposes. As summarized in Table 1, when no catalyst was present (entry 1, Table 1) or light (entry 2, Table 1), only limited yields of 18%−20% were observed for the desired product (2a, Scheme 2). Interestingly, RGO shows an intrinsic catalytic activity (yield of 25%) in this reaction (entry 3, Table 1), which may contribute (at least in part) to the enhanced catalytic performances of the RGO−EY. As a comparison, the homogeneous EY shows obvious photo-catalytic activity at room temperature (with 42% yield and 66% selectivity) for the aerobic oxidation of ethyl α-bromo(phenyl)acetate (entry 4, Table 1). However, compared with transition metal complexes, Eosin Y always shows lower catalyst efficiency, which is attributed to its intrinsic catalytic activity.[27,54,55] After immobilization on RGO (entry 5, Table 1), to our surprise, the EY shows identical selectivity and enhanced catalytic activity, with a yield of 50% for the desired product achieved.

Besides the contribution of the RGO, the enhanced activity may be explained by the site-isolation of immobilized EY, as

well as the changes in the electron cloud density of the active sites after covalently functionalization.[56] In addition, with distinctive two-dimensional structure and intriguing properties, graphene provides a promising support to anchor photocatalyst. The particular two-dimensional structure and well dispersibility in DMA (Figure S6, Supporting Information) can reduce the mass transfer resistance, and the reactants and products can easily access and leave the active sites on both sides.[57] Considering Eosin Y is photoexcited at 490 nm[58] where RGO should show high light transmittance,[47,59] the influence of RGO on the photoexcitation of Eosin Y should be limited. The unique electronic property of graphene may also facilitate the electron transport in photocatalysis, decreasing the noneffective de-excitation of photoexcited EY.[60] Notably, as shown in Figure 5, the RGO−EY catalyst shows excellent stability upon reuse. It can maintain its catalytic performances for at least successive five cycles without obvious decline in its activity. The SEM images of RGO−EY before and after the recyclable testing showed no obvious structural change, revealing an excellent stability of the supported catalyst (Figure S7, Supporting Information). The excellent reusability and stability is probably ascribed to the covalent bonding of EY on RGO and the remarkable mechanical strength of graphene.

The performance of RGO−EY in the aerobic photo-oxidation of different benzyl halides were also investigated, and the results are summarized in Table 2. It should be noted that the RGO−EY showed comparable photocatalytic abilities with homogeneous EY (Table S2, Supporting Information).

CONCLUSIONS

In summary, we developed a facile and efficient strategy to immobilize Eosin Y on reduced graphene oxide and reveal its excellent photocatalytic performances in the aerobic oxidation of benzyl halides at room temperature. We also demonstrated that the EY immobilized on graphene could be readily recycled and reused without obvious loss of its catalytic activity. These results reveal that graphene is a promising support for anchoring of organic dyes as metal-free visible light photoredox catalysts.

ASSOCIATED CONTENT

Ⓢ Supporting Information

FTIR spectrum of RGO, FTIR spectrum of EY, C 1s XPS spectra of RGO−NH2 and RGO−EY, SEM image of RGO−EY and corresponding quantitative EDS mapping of N, O and Br, EDS spectrum of RGO−EY, element atomic ratio of Br in the final RGO−EY is 0.59%, presenting an EY loading content of 0.12 mmol·g^{-1}, image of Tyndall effect exhibited by a RGO−EY dispersion in DMA, SEM images of RGO−EY and RGO−EY after recyclable testing, synthesis of α-aryl carbonyl compounds from Eosin Y and TEM image of RGO−EY. This material is available free of charge via the Internet at http://pubs.acs.org.

AUTHOR INFORMATION

Corresponding Author

*X. Fan. Tel./Fax: +86 22-27408778. E-mail: xiaobinfan@tju.edu.cn

Notes

The authors declare no competing financial interest.

REFERENCES

(1) Yoon, T. P.; Ischay, M. A.; Du, J. Visible light photocatalysis as a greener approach to photochemical synthesis. *Nat. Chem.* **2010**, *2*, 527−532.

(2) Nagib, D. A.; MacMillan, D. W. Trifluoromethylation of arenes and heteroarenes by means of photoredox catalysis. *Nature* **2011**, *480*, 224−228.

(3) Narayanam, J. M.; Stephenson, C. R. Visible light photoredox catalysis: Applications in organic synthesis. *Chem. Soc. Rev.* **2011**, *40*, 102−113.

(4) Prier, C. K.; Rankic, D. A.; MacMillan, D. W. Visible light photoredox catalysis with transition metal complexes: Applications in organic synthesis. *Chem. Rev.* **2013**, *113*, 5322−5363.

(5) Zuo, Z.; Ahneman, D. T.; Chu, L.; Terrett, J. A.; Doyle, A. G.; MacMillan, D. W. Dual catalysis. Merging photoredox with nickel catalysis: Coupling of alpha-carboxyl sp³-carbons with aryl halides. *Science* **2014**, *345*, 437−440.

(6) Karunakaran, C.; Gomathisankar, P. Solvothermal synthesis of CeO₂−TiO₂ nanocomposite for visible light photocatalytic detoxification of cyanide. *ACS Sustainable Chem. Eng.* **2013**, *1*, 1555−1563.

(7) Zhang, Y.; Zhang, N.; Tang, Z.-R.; Xu, Y.-J. A unique silk mat-like structured Pd/CeO₂ as an efficient visible light photocatalyst for green organic transformation in water. *ACS Sustainable Chem. Eng.* **2013**, *1*, 1258−1266.

(8) Narayanam, J. M.; Tucker, J. W.; Stephenson, C. R. Electron-transfer photoredox catalysis: Development of a tin-free reductive dehalogenation reaction. *J. Am. Chem. Soc.* **2009**, *131*, 8756−8757.

(9) Nguyen, J. D.; D'Amato, E. M.; Narayanam, J. M.; Stephenson, C. R. Engaging unactivated alkyl, alkenyl and aryl iodides in visible-light-mediated free radical reactions. *Nat. Chem.* **2012**, *4*, 854−859.

(10) Chen, Y.; Kamlet, A. S.; Steinman, J. B.; Liu, D. R. A biomolecule-compatible visible-light-induced azide reduction from a DNA-encoded reaction-discovery system. *Nat. Chem.* **2011**, *3*, 146−153.

(11) Larraufie, M. H.; Pellet, R.; Fensterbank, L.; Goddard, J. P.; Lacote, E.; Malacria, M.; Ollivier, C. Visible-light-induced photo-reductive generation of radicals from epoxides and aziridines. *Angew. Chem., Int. Ed.* **2011**, *50*, 4463−4466.

(12) Tucker, J. W.; Narayanam, J. M.; Shah, P. S.; Stephenson, C. R. Oxidative photoredox catalysis: Mild and selective deprotection of PMB ethers mediated by visible light. *Chem. Commun.* **2011**, *47*, 5040−5042.

(13) Zou, Y. Q.; Chen, J. R.; Liu, X. P.; Lu, L. Q.; Davis, R. L.; Jorgensen, K. A.; Xiao, W. J. Highly efficient aerobic oxidative hydroxylation of arylboronic acids: Photoredox catalysis using visible light. *Angew. Chem., Int. Ed.* **2012**, *51*, 784−788.

(14) Maity, S.; Zheng, N. A visible-light-mediated oxidative C-N bond formation/aromatization cascade: Photocatalytic preparation of N-arylindoles. *Angew. Chem., Int. Ed.* **2012**, *51*, 9562−9566.

(15) Zhu, S.; Das, A.; Bui, L.; Zhou, H.; Curran, D. P.; Rueping, M. Oxygen switch in visible-light photoredox catalysis: Radical additions and cyclizations and unexpected C-C-bond cleavage reactions. *J. Am. Chem. Soc.* **2013**, *135*, 1823−1829.

(16) Du, J.; Skubi, K. L.; Schultz, D. M.; Yoon, T. P. A dual-catalysis approach to enantioselective [2 + 2] photocycloadditions using visible light. *Science* **2014**, *344*, 392−396.

(17) Ischay, M. A.; Ament, M. S.; Yoon, T. P. Crossed intermolecular [2+2] cycloaddition of styrenes by visible light photocatalysis. *Chem. Sci.* **2012**, *3*, 2807−2811.

(18) Nicewicz, D. A.; MacMillan, D. W. Merging photoredox catalysis with organocatalysis: the direct asymmetric alkylation of aldehydes. *Science* **2008**, *322*, 77−80.

(19) Melchiorre, P. Light in aminocatalysis: The asymmetric intermolecular alpha-alkylation of aldehydes. *Angew. Chem., Int. Ed.* **2009**, *48*, 1360−1363.

(20) McNally, A.; Prier, C. K.; MacMillan, D. W. Discovery of an alpha-amino C-H arylation reaction using the strategy of accelerated serendipity. *Science* **2011**, *334*, 1114−1117.

(21) Pirnot, M. T.; Rankic, D. A.; Martin, D. B.; MacMillan, D. W. Photoredox activation for the direct beta-arylation of ketones and aldehydes. *Science* **2013**, *339*, 1593−1596.

(22) Ohkubo, K.; Mizushima, K.; Iwata, R.; Fukuzumi, S. Selective photocatalytic aerobic bromination with hydrogen bromide via an electron-transfer state of 9-mesityl-10-methylacridinium ion. *Chem. Sci.* **2011**, *2*, 715−722.

(23) Pan, Y. H.; Kee, C. W.; Chen, L.; Tan, C. H. Dehydrogenative coupling reactions catalysed by Rose Bengal using visible light irradiation. *Green Chem.* **2011**, *13*, 2682−2685.

(24) Pitre, S. P.; McTiernan, C. D.; Ismaili, H.; Scaiano, J. C. Mechanistic insights and kinetic analysis for the oxidative hydroxylation of arylboronic acids by visible light photoredox catalysis: A metal-free alternative. *J. Am. Chem. Soc.* **2013**, *135*, 13286−13289.

(25) Ravelli, D.; Fagnoni, M.; Albini, A. Photoorganocatalysis. What for? *Chem. Soc. Rev.* **2013**, *42*, 97−113.

(26) Nicewicz, D. A.; Nguyen, T. M. Recent applications of organic dyes as photoredox catalysts in organic synthesis. *ACS Catal.* **2014**, *4*, 355−360.

(27) Hari, D. P.; Konig, B. Eosin Y catalyzed visible light oxidative C-C and C-P bond formation. *Org. Lett.* **2011**, *13*, 3852−3855.

(28) Hari, D. P.; Schroll, P.; Konig, B. Metal-free, visible-light-mediated direct C-H arylation of heteroarenes with aryl diazonium salts. *J. Am. Chem. Soc.* **2012**, *134*, 2958−2961.

(29) Neumann, M.; Fuldner, S.; Konig, B.; Zeitler, K. Metal-free, cooperative asymmetric organophotoredox catalysis with visible light. *Angew. Chem., Int. Ed.* **2011**, *50*, 951−954.

(30) Majek, M.; von Wangelin, A. J. Organocatalytic visible light mediated synthesis of aryl sulfides. *Chem. Commun.* **2013**, *49*, 5507−5509.

(31) Yang, X. J.; Chen, B.; Zheng, L. Q.; Wu, L. Z.; Tung, C. H. Highly efficient and selective photocatalytic hydrogenation of functionalized nitrobenzenes. *Green Chem.* **2014**, *16*, 1082−1086.

(32) Hari, D. P.; Konig, B. Synthetic applications of Eosin Y in photoredox catalysis. *Chem. Commun.* **2014**, *50*, 6688−6699.

(33) Liu, X.; Li, Y.; Peng, S.; Lu, G.; Li, S. Photocatalytic hydrogen evolution under visible light irradiation by the polyoxometalate α-$[AlSiW_{11}(H_2O)O_{39}]^{5-}$-Eosin Y system. *Int. J. Hydrogen Energy* **2012**, *37*, 12150−12157.

(34) Liu, X.; Li, Y.; Peng, S.; Lu, G.; Li, S. Photosensitization of $SiW_{11}O_{39}{}^{8-}$-modified TiO_2 by Eosin Y for stable visible-light H_2 generation. *Int. J. Hydrogen Energy* **2013**, *38*, 11709−11719.

(35) Abe, R.; Hara, K.; Sayama, K.; Domen, K.; Arakawa, H. Steady hydrogen evolution from water on Eosin Y-fixed TiO_2 photocatalyst using a silane-coupling reagent under visible light irradiation. *J. Photochem. Photobiol., A* **2000**, *137*, 63−69.

(36) Chatterjee, D.; Mahata, A. Demineralization of organic pollutants on the dye modified TiO_2 semiconductor particulate system using visible light. *Appl. Catal., B* **2001**, *33*, 119−125.

(37) Gazi, S.; Ananthakrishnan, R. Metal-free-photocatalytic reduction of 4-nitrophenol by resin-supported dye under the visible irradiation. *Appl. Catal., B* **2011**, *105*, 317−325.

(38) Li, Y.; Xie, C.; Peng, S.; Lu, G.; Li, S. Eosin Y-sensitized nitrogen-doped TiO_2 for efficient visible light photocatalytic hydrogen evolution. *J. Mol. Catal. A: Chem.* **2008**, *282*, 117−123.

(39) Li, Y.; Guo, M.; Peng, S.; Lu, G.; Li, S. Formation of multilayer-Eosin Y-sensitized TiO_2 via Fe^{3+} coupling for efficient visible-light

photocatalytic hydrogen evolution. *Int. J. Hydrogen Energy* **2009**, *34*, 5629−5636.

(40) Novoselov, K. S.; Geim, A. K.; Morozov, S. V.; Jiang, D.; Zhang, Y.; Dubonos, S. V.; Grigorieva, I. V.; Firsov, A. A. Electric field effect in atomically thin carbon films. *Science* **2004**, *306*, 666−669.

(41) Geim, A. K.; Novoselov, K. S. The rise of graphene. *Nat. Mater.* **2007**, *6*, 183−191.

(42) Jin, X.; Dang, L.; Lohrman, J.; Subramaniam, B.; Ren, S.; Chaudhari, R. V. Lattice-matched bimetallic CuPd-graphene nanocatalysts for facile conversion of biomass-derived polyols to chemicals. *ACS Nano* **2013**, *7*, 1309−1316.

(43) Hong, C.; Jin, X.; Totleben, J.; Lohrman, J.; Harak, E.; Subramaniam, B.; Chaudhari, R. V.; Ren, S. Graphene oxide stabilized Cu_2O for shape selective nanocatalysis. *J. Mater. Chem. A* **2014**, *2*, 7147.

(44) Lee, C.; Wei, X.; Kysar, J. W.; Hone, J. Measurement of the elastic properties and intrinsic strength of monolayer graphene. *Science* **2008**, *321*, 385−388.

(45) Das Sarma, S.; Adam, S.; Hwang, E. H.; Rossi, E. Electronic transport in two-dimensional graphene. *Rev. Mod. Phys.* **2011**, *83*, 407−470.

(46) Kim, K. S.; Zhao, Y.; Jang, H.; Lee, S. Y.; Kim, J. M.; Kim, K. S.; Ahn, J. H.; Kim, P.; Choi, J. Y.; Hong, B. H. Large-scale pattern growth of graphene films for stretchable transparent electrodes. *Nature* **2009**, *457*, 706−710.

(47) Bonaccorso, F.; Sun, Z.; Hasan, T.; Ferrari, A. C. Graphene photonics and optoelectronics. *Nat. Photonics* **2010**, *4*, 611−622.

(48) Huang, X.; Qi, X.; Boey, F.; Zhang, H. Graphene-based composites. *Chem. Soc. Rev.* **2012**, *41*, 666−686.

(49) Mou, Z. G.; Dong, Y. P.; Li, S. J.; Du, Y. K.; Wang, X. M.; Yang, P.; Wang, S. D. Eosin Y functionalized graphene for photocatalytic hydrogen production from water. *Int. J. Hydrogen Energy* **2011**, *36*, 8885−8893.

(50) Zhang, W.; Li, Y.; Peng, S.; Cai, X. Enhancement of photocatalytic H_2 evolution of eosin Y-sensitized reduced graphene oxide through a simple photoreaction. *Beilstein J. Nanotechnol.* **2014**, *5*, 801−811.

(51) Wang, S. S.; Wang, J.; Zhang, W. F.; Ji, J. Y.; Li, Y.; Zhang, G. L.; Zhang, F. B.; Fan, X. B. Ethylenediamine modified graphene and its chemically responsive supramolecular hydrogels. *Ind. Eng. Chem. Res.* **2014**, *53*, 13205−13209.

(52) Zhu, Y. W.; Murali, S.; Stoller, M. D.; Velamakanni, A.; Piner, R. D.; Ruoff, R. S. Microwave assisted exfoliation and reduction of graphite oxide for ultracapacitors. *Carbon* **2010**, *48*, 2118−2122.

(53) Ferrari, A. C.; Meyer, J. C.; Scardaci, V.; Casiraghi, C.; Lazzeri, M.; Mauri, F.; Piscanec, S.; Jiang, D.; Novoselov, K. S.; Roth, S.; Geim, A. K. Raman spectrum of graphene and graphene layers. *Phys. Rev. Lett.* **2006**, *97*, 187401.

(54) Condie, A. G.; Gonzalez-Gomez, J. C.; Stephenson, C. R. Visible-light photoredox catalysis: aza-Henry reactions via C-H functionalization. *J. Am. Chem. Soc.* **2010**, *132*, 1464−1465.

(55) Su, Y.; Zhang, L.; Jiao, N. Utilization of natural sunlight and air in the aerobic oxidation of benzyl halides. *Org. Lett.* **2011**, *13*, 2168−2171.

(56) Wegener, S. L.; Marks, T. J.; Stair, P. C. Design strategies for the molecular level synthesis of supported catalysts. *Acc. Chem. Res.* **2012**, *45*, 206−214.

(57) Ji, J.; Zhang, G.; Chen, H.; Wang, S.; Zhang, G.; Zhang, F.; Fan, X. Sulfonated graphene as water-tolerant solid acid catalyst. *Chem. Sci.* **2011**, *2*, 484.

(58) De, S.; Das, S.; Girigoswami, A. Environmental effects on the aggregation of some xanthene dyes used in lasers. *Spectrochim. Acta, Part A* **2005**, *61*, 1821−1833.

(59) T.K, B. S.; Nair, A. B.; Abraham, B. T.; Beegum, P. M. S.; Thachil, E. T. Microwave exfoliated reduced graphene oxide epoxy nanocomposites for high performance applications. *Polymer* **2014**, *55*, 3614−3627.

(60) Min, S.; Lu, G. Dye-sensitized reduced graphene oxide photocatalysts for highly efficient visible-light-driven water reduction. *J. Phys. Chem. C* **2011**, *115*, 13938−13945.